17th World Conference on Earthquake Engineering, 17WCEE

Sendai, Japan - September 13th to 18th 2020

VISCOUS DAMPER OPTIMIZATION CONSIDERING PRACTICAL DESIGN ISSUES

D. Lopez-Garcia[(1)(2)], F. Saitua[(3)], A. A. Taflanidis[(4)]

[(1)] *Associate Professor, Department of Structural & Geotechnical Engineering, Pontificia Universidad Catolica de Chile, dlg@ing.puc.cl*
[(2)] *Researcher, Research Center for Integrated Disaster Risk Management (CIGIDEN) ANID FONDAP 15110017 (Chile)*
[(3)] *Structural Engineer, Rene Lagos Engineers, fesaitua@gmail.com*
[(4)] *Associate Professor, Department of Civil & Environmental Engineering & Earth Sciences, University of Notre Dame, a.taflanidis@nd.edu*

Abstract

This research discusses the optimal height-wise distribution of viscous dampers in multistory structures considering practical design issues, all quantified with respect to the implementation cost. Seismic excitation is modeled as a stochastic process (filtered white noise), and response statistics of linear structural systems are obtained through state-space analysis. For applications involving nonlinear dampers, statistical linearization principles are employed to approximate damper and structural response. Emphasis is placed on three practical design issues: (i) realistic quantification of damper upfront cost, based on damper force capacity rather than merely on damping coefficients; (ii) explicit incorporation (into the optimization procedure) of the cost of column strengthening that might be required to accommodate the additional forces (with respect to those on the bare structure) due to the action of the supplemental dampers; and (iii) the maximum feasible force capacity of the dampers. Five different objective functions are defined to address these issues, all of them incorporating cost characteristics (for dampers and strengthening) at different fidelity levels. The impact of the statistical linearization when the objective function is defined in terms of peak response quantities (instead of RMS quantities) is discussed. The optimal design problem considers primarily the structural performance as a constraint, requiring that a specific level of vibration suppression be achieved (with respect to the structural response without dampers) through the damper implementation. The proposed framework is illustrated through the design of a supplemental viscous damping system for an actual Chilean 26-story building, considering an excitation that is compatible with the regional seismic hazard. Results demonstrate that explicitly optimizing for cost functions that consider practical design issues leads to substantial economic benefits with respect to optimization for simplified cost metrics.

Keywords: viscous damper optimization; stochastic excitation; multi-objective optimization

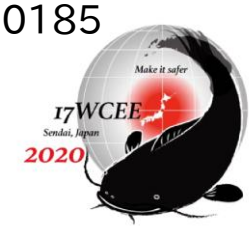

1. Introduction

Fluid viscous dampers are an attractive seismic protection device for new and existing buildings [1]. Their effectiveness in reducing the seismic response of multistory buildings is sensitive to their chosen distribution [2, 3], and a variety of optimization approaches, considering different performance quantifications and modeling assumptions, have been developed for this task [4-11]. They range from approaches utilizing simple schemes, distributing total damping coefficient according to pre-selected simplified criteria, with the total damping coefficient chosen so that a specific performance is achieved, to approaches that establish a formal optimization procedure based on some chosen performance objectives. Simplified approaches adopt a modal analysis philosophy, emphasizing the damping ratio (or transfer function) at the fundamental mode. Other methodologies use time-history analysis and peak response quantities to evaluate structural performance. Between these two extremes in terms of complexity, another wide range of approaches evaluate performance using random vibration theory, modeling the seismic excitation as a stationary stochastic process.

This study investigates the optimal height-wise distribution of viscous dampers in multistory structures with emphasis on design considerations that are relevant in practical applications but have not been yet fully explored in past studies. Since intent is to address practical applications, a damper distribution approach appropriate for such a setting is adopted, avoiding unnecessary modeling complexity that might reduce the applicability, for example need to examine a small only number of devices [10] (i.e. have a small only number of design variables in the design optimization to accommodate for the complexity stemming from the adoption of complex models for describing structural performance). This is facilitated by modeling structural performance through stationary response statistics. Within this context, the main topics addressed are: the force demand on the supplemental dampers, the cost of the supplemental dampers, and the forces on structural members due to the supplemental damping system. Though the importance of explicitly incorporating the upfront damper cost has been demonstrated in studies relying on advanced numerical modeling of structural behavior [10, 11], this cost is commonly ignored, or is only approximately addressed, in simplified design frameworks like the one considered here. In these latter cases usually the total damping coefficient is considered [2], but this quantity does not explicitly indicate the damper cost, which is actually more related to the force capacity rather than to the damping coefficient.

2. Equations of motion and space-state representation

2.1 State-space formulation

Consider a n_s-story building equipped with n_d viscous dampers (linear or nonlinear) connecting adjacent (i.e., consecutive) floor levels. Let $\mathbf{x}_s \in \Re^{n_s}$ be the vector of floor displacements of the primary structure relative to the ground and $\ddot{x}_g \in \Re$ be the ground acceleration. The equation of motion of the structure is given by:

$$\mathbf{M}_s \ddot{\mathbf{x}}_s(t) + \mathbf{C}_s \dot{\mathbf{x}}_s(t) + \mathbf{K}_s \mathbf{x}_s(t) + \mathbf{T}_d^T \mathbf{f}_d(t) = -\mathbf{M}_s \mathbf{R}_s \ddot{x}_g(t) \tag{1}$$

where $\mathbf{M}_s \in \Re^{n_s \mathrm{x} n_s}$, $\mathbf{C}_s \in \Re^{n_s \mathrm{x} n_s}$, and $\mathbf{K}_s \in \Re^{n_s \mathrm{x} n_s}$ are the mass, damping, and stiffness matrices of the primary structure, respectively, $\mathbf{R}_s \in \Re^{n_s}$ is the earthquake influence coefficient vector (vector of ones), $\mathbf{f}_d \in \Re^{n_d}$ is the vector of damper forces and $\mathbf{T}_d \in \Re^{n_d \mathrm{x} n_s}$ is the connectivity matrix that relates the velocities of the global degrees of freedom to the vector of relative velocities between the ends of each damper so that $\dot{\mathbf{v}} = \mathbf{T}_d \dot{\mathbf{x}}_s$, where $\dot{\mathbf{v}}$ stands for the damper relative velocities. Let $\ddot{x}_g$ be modeled as a stationary filtered Gaussian white noise stochastic process. A state-space formulation is utilized to determine the response statistics. In this setting, the excitation model is:

$$\dot{\mathbf{x}}_q(t) = \mathbf{A}_q \mathbf{x}_q(t) + \mathbf{E}_q w(\mathrm{t}); \quad \ddot{x}_g(t) = \mathbf{C}_q \mathbf{x}_q(t) \tag{2}$$

where $w(t) \in \Re$ is a zero-mean Gaussian white-noise process with spectral intensity equal to $S_w = 1/(2\pi)$; $\mathbf{x}_q(t) \in \Re^{n_q}$ is the state vector for the excitation; $\mathbf{A}_q \in \Re^{n_q \mathrm{x} n_q}$, $\mathbf{E}_q \in \Re^{n_q \mathrm{x} 1}$ and $\mathbf{C}_q \in \Re^{1 \mathrm{x} n_q}$ are the state-space

excitation matrices. Combining excitation model of Eq. (2) with the equations of motion of the structural system (Eq. (1)) provides the augmented state-space system:

$$\dot{\mathbf{x}}(t) = \mathbf{A}\mathbf{x}(t) + \mathbf{B}\mathbf{f}_d(t) + \mathbf{E}w(t);\ \ \mathbf{z}(t) = \mathbf{C}\mathbf{x}(t) + \mathbf{D}\mathbf{f}_d(t) \tag{3}$$

where $\mathbf{x}(t) \in \Re^{n_x}$ is the state vector with $n_x = 2n_s + n_q$; $\mathbf{z}(t) \in \Re^{n_z}$ is the vector of performance variables (response output of the system) with z_i denoting the i^{th} output; and **A**, **B, E**, **C, D** are the system state-space matrices. Note that the proposed formulation takes into account the spectral characteristics of the stochastic excitation by appropriate augmentation of the state equation [12]. The derivation of the state space matrices is discussed in the Appendix.

The force demand on the *i*-th viscous damper of the system is given by $f_{di} = c_{di}\left|\dot{v}_i\right|^{\alpha_i}\mathrm{sgn}(\dot{v}_i)$ where α_i, c_{di} and $\dot{v}_i$ are the viscous exponent, damping coefficient and relative velocity of the *i*-th viscous damper, and sgn(.) is the signum function. For linear dampers $\alpha_i = 1$ whereas for nonlinear dampers statistical linearization can be employed to replace the nonlinear force with an equivalent linear one. In this case, the equivalent damping coefficient of the *i*-th viscous damper c_{eqi} is given by [13]:

$$c_{eqi} = c_{di}\frac{2^{1+\frac{\alpha_i}{2}}\Gamma(1+\frac{\alpha_i}{2})}{\sqrt{2\pi}}\sigma_{\dot{v}i}^{\alpha_i - 1} \tag{4}$$

where $\Gamma(.)$ is the Gamma function and $\sigma_{\dot{v}i}$ is the standard deviation of $\dot{v}_i$. The linearized damper force is then $f_{di} = c_{eqi}\dot{v}_i$. The damper force vector $\mathbf{f}_d$, with elements f_{di}, can be expressed as $\mathbf{f}_d = \mathbf{K}(\mathbf{c}_{eq})\dot{\mathbf{v}}$ where $\mathbf{K}(\mathbf{c}_{eq})$ is a diagonal matrix with the equivalent damping coefficient c_{eqi} of each damper. Relative velocities are given by $\dot{\mathbf{v}} = \mathbf{T}_d\dot{\mathbf{x}}_s = \mathbf{L}_d\mathbf{x}$, where $\mathbf{L}_d$ is the state connectivity matrix that relates these velocities to the state vector, also given in the Appendix, and the dependence of **K** on $\mathbf{c}_{eq}$ is explicitly emphasized. We can finally formulate the final state-space system representation:

$$\dot{\mathbf{x}}(t) = \mathbf{A}_a(\mathbf{c}_{eq})\mathbf{x}(t) + \mathbf{E}w(t);\ \ \mathbf{z}(t) = \mathbf{C}_a(\mathbf{c}_{eq})\mathbf{x}(t)$$

where (5)

$$\mathbf{A}_a(\mathbf{c}_{eq}) = \mathbf{A} + \mathbf{B}\mathbf{K}(\mathbf{c}_{eq})\mathbf{L}_d;\ \mathbf{C}_a(\mathbf{c}_{eq}) = \mathbf{C} + \mathbf{D}\mathbf{K}(\mathbf{c}_{eq})\mathbf{L}_d.$$

2.2 Response statistics estimation

Under the modelling assumptions discussed above, the output of the system, $\mathbf{z}(t)$, has a Gaussian distribution with zero mean and covariance matrix in stationary response given as

$$\mathbf{K}_{\mathbf{zz}} = \mathbf{C}_a(\mathbf{c}_{eq})\mathbf{P}(\mathbf{c}_{eq})\mathbf{C}_a(\mathbf{c}_{eq})^T;\ \ \mathbf{A}_a(\mathbf{c}_{eq})\mathbf{P}(\mathbf{c}_{eq}) + \mathbf{P}(\mathbf{c}_{eq})\mathbf{A}_a(\mathbf{c}_{eq})^T + \mathbf{E}\mathbf{E}^{\mathrm{T}} = 0 \tag{6}$$

where $\mathbf{P}(\mathbf{c}_{eq})$ corresponds to the state covariance matrix, obtained, as shown above, by the solution of an algebraic Lyapunov equation [14]. The variance of each of the n_z system output variables is given by the corresponding element of the diagonal of $\mathbf{K}_{zz}$. The variances of the damper relative velocities are also needed in the problem formulation and are related to the state covariance matrix by:

$$\boldsymbol{\sigma}_{\dot{\mathbf{v}}}^2 = \mathbf{L}_d^T\mathbf{P}(\mathbf{c}_{eq})\mathbf{L}_d \tag{7}$$

Using these variances, the RMS damper forces can be obtained as:

$$\boldsymbol{\sigma}_{\mathbf{f}_d} = \mathbf{K}(\mathbf{c}_{eq})\boldsymbol{\sigma}_{\dot{\mathbf{v}}} \tag{8}$$

When statistical linearization is employed, variances $\boldsymbol{\sigma}_{\dot{\mathbf{v}}}^2$ are also used to calculate the equivalent damping coefficient given by Eq. (4). In this case a cyclic dependence exists: c_{eqi} depends on $\sigma_{\dot{v}i}$ based on Eq. (4), but based on Eq. (7) and the dependence on $\mathbf{P}(\mathbf{c}_{eq})$, the latter also depends (implicitly) on c_{eqi}. An iterative process is therefore needed to solve for the equivalent damper coefficients and the state covariance matrix. In the context of the optimization established later in this study this is avoided by adopting the equivalent damping coefficients as the primary design variables, and then back-deriving the actual damping coefficients. In this case there is no iterative process required. Once c_{eqi} is known, $\sigma_{\dot{v}i}$ can be solved for by calculating the second order statistics, and finally c_{di} can be computed using Eq. (4).

3. Cost-based optimal damper distribution

The design objective is to identify the optimal damping coefficient vector $\mathbf{c}_d$ made up of the damper coefficients of all supplemental dampers. To simplify the optimization, the equivalent damping coefficient is posed as the design optimization vector as discussed earlier, and then Eq. (4) is applied to determine $\mathbf{c}_d$ (note that if dampers are linear, $\mathbf{c}_d = \mathbf{c}_{eq}$). Design objectives are related to the cost of implementation of the supplemental damping system whereas considerations about the established vibration suppression level are incorporated through performance constraints.

3.1 Cost-based objective functions

Three different cost functions are considered. The first and simplest one is the sum of RMS damper forces, i.e.:

$$J_1(\mathbf{c}_{eq}) = \sum_{i=1}^{n_d} \sigma_{f_d i} \tag{9}$$

where $\sigma_{f_d i}$ is the RMS force demand on the i-th damper, given by components of vector in Eq. (8), and J_1 has units of force. This measure facilitates a closer connection to the damper cost [10] than the commonly adopted [2] total damping coefficient C_o (sum of each damping coefficient c_{di}). However, damper cost is actually related to damper force capacity, which is a function of the *peak* damper force rather than of the RMS response. Moreover, this cost is not linearly related to damper force capacity [10]. The second cost function incorporates these considerations, and is given by:

$$J_2(\mathbf{c}_{eq}) = 96.88 \sum_{i=1}^{n_d} f_{doi}^{0.607} \tag{10}$$

where f_{doi} is the *peak* force demand on the i-th damper (in units of kN) and J_2 is expressed in United States Dollars (USD). For linear dampers peak force quantities can be approximately related to RMS values as $f_{doi} = p_f \sigma_{f_d i}$, where p_f is the peak factor, relating the mean of the peak damper force (or peak of any stochastic variable) to its standard deviation. In this study this factor is taken as 2, corresponding to a single degree of freedom oscillator with 5% damping vibrating for 20 cycles based on up-crossing rate [15], the latter representing the period of vibration for stochastic variables. The 20 cycles were chosen to accommodate the case study considered later, based on strong ground motion duration characteristics for the region and the fundamental period of the building structure. For nonlinear dampers a modification is warranted since accuracy of statistical linearization typically reduces for peak response quantities, compared to the accuracy of average/RMS response quantities [16]. Since intent of developed framework is to have practical utility, a simplified approximation is adopted to estimate peak damper forces. These are assumed equal to the forces developed for a specific peak velocity, and therefore are given by:

$$f_{doi} = c_{di} (p_f \sigma_{\dot{v}i})^{\alpha} \tag{11}$$

A final, new cost function J_3 is introduced in this study to account for the cost of column strengthening due to the additional forces imposed by the damping system. This cost is assessed as a function of the ratio of

the additional axial load due to damper forces to the initial axial load capacity (i.e. the axial load capacity of the structure without dampers). This ratio indicates the relative degree of strengthening required. In turn, the additional axial load on columns due to damper forces is a function of the cumulative damper force (i.e., the sum of forces in dampers located above a given story). This cost function is then given by:

$$J_3(\mathbf{c}_{eq}) = 96.88 \sum_{i=1}^{n_d} f_{doi}^{0.607} + \omega_N \sum_{j=1}^{n_s} \frac{\gamma F_{Doj}}{N_{oj}} = J_2(\mathbf{c}_{eq}) + \omega_N \sum_{j=1}^{n_s} \frac{\gamma F_{Doj}}{N_{oj}} \tag{12}$$

where F_{Doj} is the peak cumulative damper force at the j-th story, N_{oj} is the initial (i.e., of the structure without dampers) axial load capacity of the columns at the j-th story and J_3 is expressed in USD. The parameter ω_N (also expressed in USD) is a constant introduced to: (i) convert damper forces to axial forces at each story (i.e., it considers the geometric variability of different damper bracing alternatives as discussed next); and (ii) quantify the cost of the strengthening required relative to the initial axial load capacity. Weight γ is a constant modification factor introduced for nonlinear dampers to approximate peak response statistics. The RMS axial force on the columns at a given story, N_{fj}, is proportional to the RMS cumulative damper force at the same story, F_{Dj}. Hence, for the sake of conceptual clarity, from now on the quantity F_D will be referred to as "axial load", with F_{Dj} representing the axial load on the columns on the (j−1)-th story (for instance, F_{D1} is the axial load over the foundation and F_{D2} the axial load over the first story columns). Peak axial forces are calculated through use of the peak factor as $F_{Doj} = p_f F_{Dj}$, whereas for nonlinear dampers a modification is established through γ to consider that statistics for F_{Doj} are based on linearization for the damper forces (peak forces approximated $f_{doi} = p_f \sigma_{f_d i}$), whereas peak damper forces are better approximated by Eq. (11). Modification factor for the axial load at each story γ is obtained by calculating the ratio of peak force under these two assumptions and is given by (dependence on i removed in this equation since final expression is independent of specific damper):

$$\gamma = \frac{c_d (p_f \sigma_{\dot{v}})^{\alpha}}{p_f \sigma_{f_d}} = \frac{p_f^{\alpha-1}\sqrt{2\pi}}{2^{1+\frac{\alpha_i}{2}}\Gamma\left(1+\frac{\alpha}{2}\right)} = \gamma(\alpha) \tag{13}$$

which is a function only of the viscous exponent α. Since this weight is same for all dampers at all stories, this modification accurately adjusts for the cumulative effect of the peak damper force at each story. For linear dampers $\gamma = 1$ whereas for nonlinear dampers $\gamma < 1$,and therefore axial load is reduced.

To evaluate N_{oj} it is assumed that column cross-sections change every n_r stories, hence so does the initial axial load capacity. The initial axial load capacity at the foundation level is assumed equal to a typical axial load on a column due to gravity loads on a typical story, denoted $\overline{N}$, multiplied by the number of stories n_s. Since, to the best of the authors' knowledge, no reliable information on the value of factor ω_N is available, a parametric analysis will be performed. For the same reason (i.e., lack of available information) the cost of column strengthening is assumed linearly related to the axial force.

Cost function J_1 relates in a simplified manner (linearly) the cost of the dampers to the damper force, and in this study is mainly considered for comparison to the more realistic, and broadly applicable, nonlinear cost function J_2. Cost function J_3 incorporates additional considerations about column strengthening, and is particularly relevant for retrofit scenarios, when supplemental damper forces needs to be balanced against the column capacities.

The relationship in Eq. (10) between the damper force capacity and the damper cost was derived from the analysis of available commercial information [10] and indicates that the cost of a marginal increment in force capacity is smaller in dampers having a large force capacity than in dampers having a small force capacity. This cost function, though, does not incorporate considerations about the maximum feasible damper force capacity $f_{\max}$ of commercially available dampers. Of course larger values of f_{doi} can be accommodated by using multiple dampers per story, with the capacities of each damper limited to $f_{\max}$. In this case, though, the

cost per damper is related to each individual force capacity and not the total capacity per story. To address this issue, the following modification, is proposed for J_2, assuming that if at some story f_{doi} exceeds $f_{\max}$ then such demand will be accommodated using multiple, equal capacity dampers, the number of which is the smallest number needed so that the force capacity of each damper is smaller than $f_{\max}$

$$J_{2m}(\mathbf{c}_{eq}) = 96.88\sum_{i=1}^{n_d}\left[\frac{f_{doi}}{f_{\max}}\right]\left(f_{doi}/\left[\frac{f_{doi}}{f_{\max}}\right]\right)^{0.607} \tag{14}$$

where [.] is the ceiling function. Similar considerations for cost function J_3 in Eq. (12) lead to J_{3m}.

3.2 Functions related to structural performance

The function incorporating structural performance considerations in the design can be described based on second order statistics of the output. Since seismic performance is typically expressed in terms of occurrence of different failure modes, quantified by engineering demand parameters exceeding certain thresholds, it is reasonable to define performance in terms of the maximum normalized variance. The latter is directly related to the probability of occurrence of any failure mode in the structure [12]. This approach leads to definition for the performance function as $h(\boldsymbol{\sigma}_z) = \max_k(\lambda_k \sigma_{zk} / \beta_k)$, where λ_k and β_k are the relative importance and normalization constant of the k-th output of $\mathbf{z}$, respectively.

3.3 Height-wise optimal distribution design problem

The optimization problem is formulated as constrained optimization with cost metric J_l (where l refers to different alternatives, J_1, J_2/J_{2m} or J_3/J_{3m}) corresponding to the objective function to be minimized and the performance function $h(\boldsymbol{\sigma}_z)$ corresponding to the constraint. At the design stage focus is placed on the interstory drift performance, leading to $\lambda_k = 0$ for performance outputs associated with accelerations and $\lambda_k = 1$ or the outputs associated with the interstory drifts. Threshold β_k is chosen same for all drifts and equal to the maximum RMS interstory drift response of the structure without dampers. This constraint selection ultimately facilitates the identification of the damper distribution providing a target reduction of the interstory drift response with respect to that of the uncontrolled structure. The optimization problem is expressed as:

$$\mathbf{c}_{eq}{}^{*} = \arg\min_{\mathbf{c}_{eq}\in\Re_{+}^{n_d}} J_l(\mathbf{c}_{eq}) \text{ such that } \frac{\max_j\left[\sigma_{\delta j}(\mathbf{c}_{eq})\right]}{\overline{\sigma_{\delta o}}} \le c_{tg} \tag{15}$$

where $\sigma_{\delta j}$ is the RMS interstory drift response at the j-th story of the structure equipped with dampers, $\overline{\sigma_{\delta 0}}$ is the maximum RMS interstory drift response (over all stories) of the structure without dampers and c_{tg} is the target performance, representing the vibration suppression ratio with respect to the uncontrolled structure. This optimization problem corresponds to a nonlinear constrained optimization problem with potentially multiple local minima (non-convex characteristics). The challenges in this optimization problem stem from multiple sources: nonlinearities in the objective functions and constraints (use of max function for the latter creates a non-smooth problem), and trade-off in the performance between the capacity of dampers at different floors. To address these challenges a global optimization algorithm is adopted and implemented through the TOMLAB optimization environment [17].

Should be pointed out that in the case of nonlinear dampers, cost function J_1 does not change in the sense that linear and nonlinear damper distributions having the same values of c_{eqi} (equal to c_{di} for linear dampers) lead to the same value of J_1. Objective functions J_2, J_{2m}, J_3 and J_{3m}, though, do take different values depending on whether dampers are a linear or nonlinear. The difference stems from the modification established to calculate the peak damper force given by Eq. (11). If this modification was not established, and peak forces were calculated using direct statistical linearization, no differences would exist.

4. Case study

The design framework is illustrated next for the retrofit of an existing 26-story Chilean building [18] with viscous dampers. The chosen building, having base dimensions of 18 by 23 meters, total seismic weight of 11690 tonf and typical story-height of 2.52 meters, is a typical example of Chilean residential high-rise building (in terms of structural properties and modal characteristics). Five different design cases are examined with respect to the objective function definition, J_1, J_2, J_{2m}, J_3 or J_{3m}, and will be referenced, respectively, as D_1, D_2, D_{2m}, D_3 and D_{3m}. The target reduction of interstory drift response is set equal to 40%, i.e., c_{tg} chosen as 0.60. Based on commercially available data maximum force capacity $f_{\max}$ of a single damper is set equal to 815 tonf. Note that tonf is used herein to describe forces, as is the standard in the Chilean region. Conversion to kN, if desired, can be established by multiplying given force values by g constant.

4.1 Structural and excitation models

Two 2D models are developed for the structure (one along each of the two main orthogonal axes x and y), obtained by static condensation of the initial 3D structural model. The degrees of freedom of the resulting 2D models are the lateral floor displacements of each of the 26 storys. The 2D models are denoted 26X and 26Y, respectively, and their first and second vibration periods are 1.29 sec, 0.30 sec, in the x direction and 1.51 sec, 0.35 sec, in the y direction. The modal participating mass ratios of the first and second mode are 0.69 and 0.18 for the 26X model, and 0.66 and 0.18 for the 26Y model. The inherent damping is assumed equal to 5% for all modes.

The stationary seismic excitation $\ddot{x}_g$ is described by a high-pass filtered Kanai-Tajimi power spectrum [19]:

$$S_g(\omega) = s_o \frac{\omega_g^4 + 4\zeta_g^2\omega^2\omega_g^2}{\left(\omega_g^2 - \omega^2\right)^2 + 4\zeta_g^2\omega_g^2\omega^2} \frac{\omega^4}{\left(\omega_f^2 - \omega^2\right)^2 + 4\zeta_f^2\omega_f^2\omega^2} . \tag{16}$$

In the above equation parameters ω_g and ζ_g represent the stiffness/frequency and damping properties, respectively, of the supporting ground modeled by a linear damped SDOF oscillator driven by white noise. Further, parameters ω_f and ζ_f control the cut-off frequency and the "steepness" of a high-pass filter used to suppress the low frequency content allowed by the Kanai-Tajimi filter. Lastly, s_o is chosen to achieve a desired value for the root mean square acceleration a_{RMS} of the considered seismic input. The parameters of the filter are chosen through calibration to a suite of ground motions that are representative of the Chilean seismic hazard. Ground motions recorded during the M_w 8.8 2010 Maule (Chile) earthquake are chosen for this purpose. From the available ground motions, only the ones recorded on what is defined as Soil Type II (soft rock or stiff soil) in the Chilean seismic design code NCh433 are considered. Soil Type II is the soil type at the location of the considered building. This calibration leads to values ω_g = 16.46 rad/s, ζ_g = 0.6, ω_f = 6.845 rad/s and ζ_f = 0.48. a_{RMS} is calculated based on a target Peak Ground Acceleration (PGA), with the latter defined based on NCh433 provisions for Seismic Zone 2 (where Santiago City is located) as 0.30g. Assuming a peak factor of 2 (same value adopted earlier), the target a_{RMS} is then 0.15g. Based on results obtained from a parametric analysis (not shown here due to space constraints) the value of factor ω_N is set equal to 1000 USD.

4.2 Results and discussion

The height-wise optimization is performed for linear dampers (α = 1) for both Models 26X and 26Y and for nonlinear dampers with α = 0.35 for Model 26X. Latter case (i.e., nonlinear dampers) will be referenced to with superscript *nl* herein. To investigate the benefits of the height-wise damper distributions given by the proposed explicit optimization approach, two other well-known height-wise distribution schemes are considered here. The first approach is the Uniform distribution, i.e., same damper capacity in all stories. The second approach is the Sequential Search Algorithm SSA [4], where dampers are placed sequentially at the story where the value of a performance index (interstory drift in this study) reaches a maximum. The

computation of the performance index is based on the second order statistics of the response. In both schemes the same target performance is adopted, i.e. reduction of drift corresponding to c_{tg}. The superscripts *U* and *SSA* are used, respectively, to describe these two simplified distributions.

Results are presented in Tables 1-3 and Fig. 1. Table 1 presents all cost functions J_l evaluated at optimal design vector for each design case; maximum peak force over all dampers max(f_{do}); damping ratio of the retrofitted structure at the fundamental mode ξ; and mean ratio per story of RMS interstory drifts $\overline{\sigma_\delta / \sigma_{\delta o}}$ and floor accelerations $\overline{\sigma_a / \sigma_{ao}}$ with respect to the RMS values of the structure without dampers. The latter quantities are representations of the average response reduction per story. Table 2 presents the cost reductions J_l / J_l^U and J_l / J_l^{SSA} with respect to the Uniform and SSA distributions offered by the explicit height-wise optimization scheme. Table 3 presents the cost reduction J_l^{nl} / J_l for the nonlinear damper implementation. In Tables 2 and 3 performance is reported for each design with respect to the corresponding cost function used in the optimization, e.g., when design case D_1 is examined the ratio of objective functions J_l / J_l^{SSA} corresponds to cost function J_1 (l=1). The height-wise distribution of the peak damper forces is shown in Fig. 1 for Model 26X.

Table 1: Response quantities of interest (linear dampers)

	Model 26X					Model26Y				
	D_1	D_2	D_{2m}	D_3	D_{3m}	D_1	D_2	D_{2m}	D_3	D_{3m}
J_1 [tonf]	2553	2829	2601	2828	2716	2126	2447	2195	2505	2376
J_2 [10^3 USD]	161	90	117	112	121	97	79	84	104	101
J_{2m} [10^3 USD]	187	165	150	166	161	142	144	131	154	142
J_3 [10^3 USD]	229	204	203	160	172	191	185	180	159	159
J_{3m} [10^3 USD]	255	279	237	215	213	237	250	226	209	199
max(f_{do}) [tonf]	1382	4775	2256	2823	2446	1706	4458	3262	2180	1890
ξ [%]	14.3	15.9	14.4	16.4	15.3	14.2	17.0	15	16	15
$\overline{\sigma_\delta / \sigma_{\delta o}}$ [%]	59	60	60	58	58	61	61	61	58	59
$\overline{\sigma_a / \sigma_{ao}}$ [%]	55	62	56	62	57	55	60	57	58	57

Note: $\overline{\sigma_\delta / \sigma_{\delta o}}$ and $\overline{\sigma_a / \sigma_{ao}}$ indicate reduction of RMS interstory drift and peak floor acceleration with respect to the RMS response of the structure without supplemental dampers

Table 2: Comparison with the Uniform and SSA damper distributions (linear dampers)

	Model 26X					Model 26Y				
	D_1	D_2	D_{2m}	D_3	D_{3m}	D_1	D_2	D_{2m}	D_3	D_{3m}
J_l/J_l^U	0.90	0.34	0.40	0.40	0.53	0.88	0.33	0.61	0.49	0.55
J_l/J_l^{SSA}	0.93	0.69	0.89	0.63	0.73	0.96	0.73	0.95	0.76	0.77

Table 3: Comparison between linear and nonlinear dampers (Model 26X)

	D_1	D_2	D_{2m}	D_3	D_{3m}
J_l^{nl}/J_l	1.00	0.84	0.84	0.80	0.76

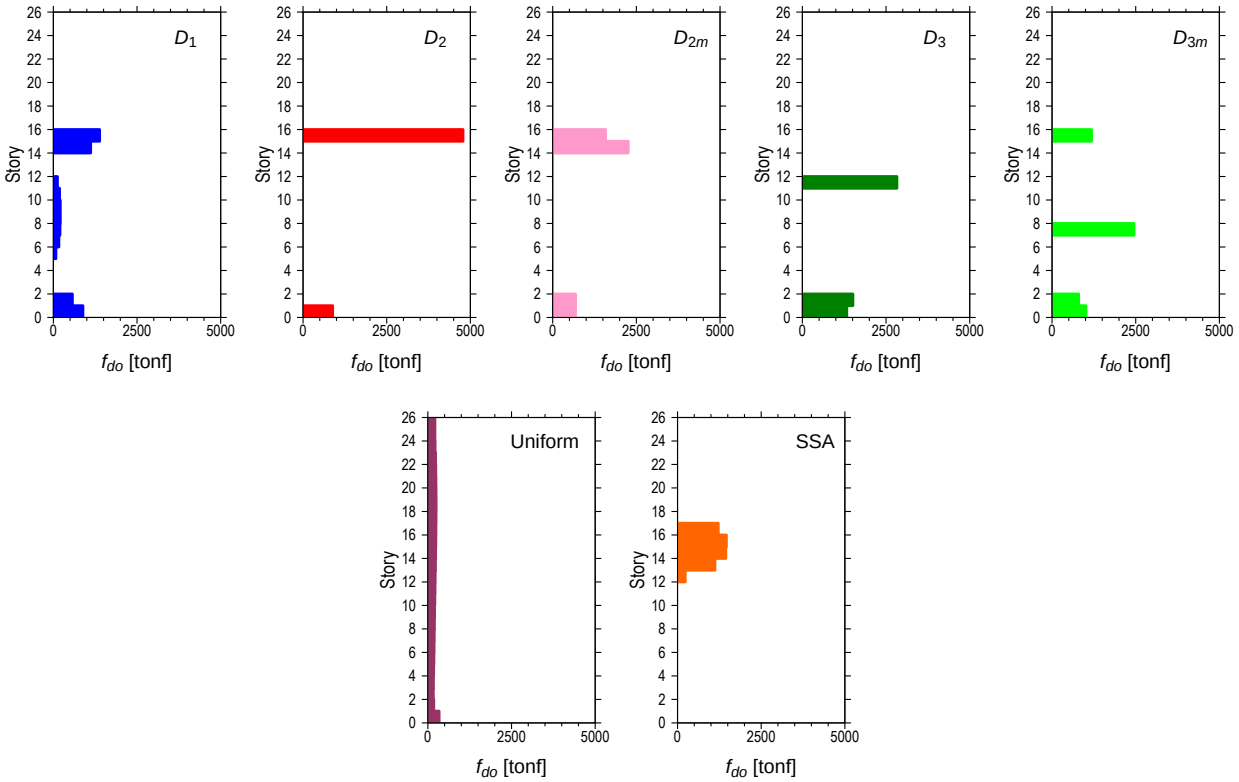

a) Linear dampers

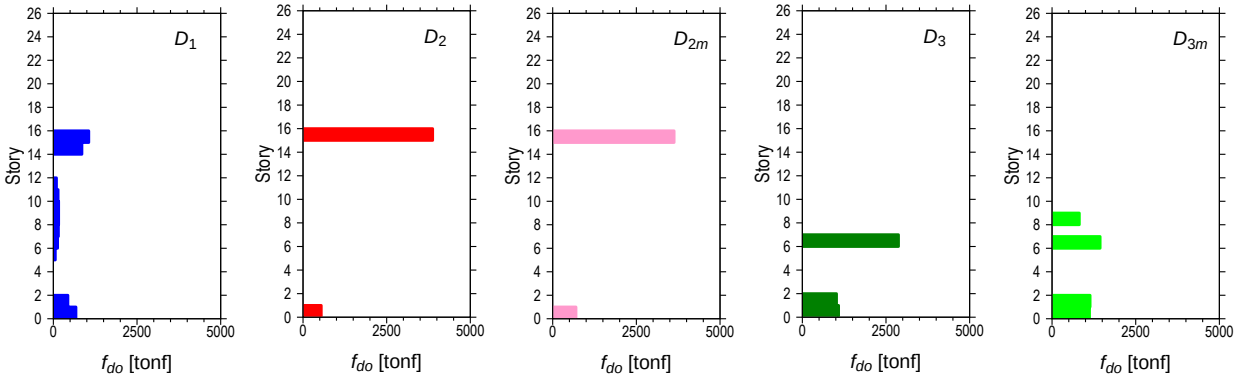

b) Nonlinear dampers

Figure 1. Peak damper forces (Model 26X)

Results show that design case D_1 minimizes force demands on dampers but at the expense of relatively large values of cost-related objectives J_2 and J_3. D_2 design leads to reductions in J_2 equal to 44% in model 26X and 18% in model 26Y, although at the expense of large values of maximum peak damper force that might not be feasible. Optimal design D_3 leads to higher values of upfront cost J_2 than D_2 but smaller values of total cost (i.e., including column strengthening) J_3. Considering both building models, J_3 is reduced on average by 24% with respect to D_1 and by 18% with respect to D_2. In the latter design cases, however, the maximum damper force max(f_{do}) exceeds the feasible limit of 815 tonf for a single damper. This means that design cases D_{2m} and D_{3m} are different from their counterpart that do not explicitly incorporate maximum force capacity considerations. Results indicate that consideration of f_{max} leads to designs having not only smaller values of J_{2m} and J_{3m} (as expected) but also smaller values of max(f_{do}). This shows that consideration of the maximum force in the damper cost leads to a distribution that avoids excessively large dampers placed at a single story.

This is also evident in Fig. 1 results. Moreover, for D_{2m} design mean floor acceleration reduction per story seems to be reduced up to 6% more with respect to is counterpart (D_2), which is another advantage of the more uniform distribution established through considering the maximum force capacity. With respect to the overall damper efficiency the results show that similar vibration suppression is established through all design cases, with the targeted reduction of 40% for maximum interstory drift established with approximately 10% of supplemental damping ratio (as intrinsic damping ratio is 5%). Such a supplemental damping threshold has been set as a reasonable objective in many viscous damper applications. With respect to the interstory drift and floor acceleration reduction, the mean drift reduction per story $\overline{\sigma_\delta / \sigma_{\delta o}}$ and mean acceleration reduction per story $\overline{\sigma_a / \sigma_{ao}}$ take similar values as the target of 40% reduction of the maximum drift. This shows that the proposed design scheme establishes a similar vibration suppression across all stories, not only at the stories where interstory drifts are maximized.

Comparison to simplified distribution schemes clearly indicates that the proposed explicit design approach leads to noticeably benefits. Differences are more noticeable when nonlinearities in the target cost function are more relevant and no constraints exist for maximum damper forces (so scheme is allowed to benefit more from an imbalanced distribution), e.g. bigger differences in the D_2 design case rather than D_{2m}. While cost is not explicitly considered in its formulation, SSA is generally more cost-effective than the Uniform distribution, most likely because, albeit simplified and sequential in nature (rather than targeting total optimality), still incorporates an explicit damper distribution based on optimality criteria and structural performance. Comparison between linear and nonlinear implementations indicates that, for a given level of structural performance, nonlinear dampers are more cost effective. Note that, as mentioned in Section 3 the value of the J_1 metric is independent of whether the dampers are linear or nonlinear (optimal distribution with respect to equivalent viscous damping is the same), which is why J_1^{nl} / J_1 ratio is equal to unity.

5. Conclusions

Cost-based optimal height-wise distributions of viscous dampers in multistory structures was investigated in this paper. Seismic excitation was modeled as a stochastic process, and response statistics were obtained through state-space analysis. Different cost functions that account (with different sophistication levels) for different relationships between cost, damper force capacity, and maximum feasible damper force capacity were considered. The performance function was defined in terms of the interstory drift response, and was used as a constraint function by imposing a target reduction of the response in comparison to the uncontrolled structure. As case study, application to a 26-story Chilean high-rise reinforced concrete building was examined. Results indicate that the explicit optimization of the damper distribution considering realistic cost metrics leads to significant savings with respect to damper distributions optimized for simplified cost metrics. Consideration of feasible damper maximum force capacity also has a significant influence on the optimal damper distribution. For nonlinear dampers it was shown, in general, that explicit consideration of nonlinearities for peak response calculation produces results that can be more cost-effective

6. Acknowledgements

Financial support was provided by the Research Center for Integrated Disaster Risk Management ANID FONDAP 15110017 (Santiago, Chile) and by CONICYT through the programs CONICYT-PCHA/MagisterNacional/2016-22161043 and Beca Ciencia y Tecnologia, Estadias Cortas 2015. The dynamic properties of the structure considered in the case study described in Section 4 were provided by VMB Ingenieria Estructural (Santiago, Chile).

7. References

[1] Symans MD, Charney FA, Whittaker AS, Constantinou MC, Kircher CA, Johnson MW, McNamara RJ (2008): Energy dissipation systems for seismic applications: current practice and recent developments. *Journal of Structural Engineering*, **134** (1), 3-21.

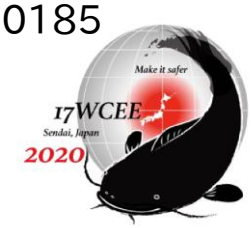

[2] Singh MP, Moreschi LM (2002): Optimal placement of dampers for passive response control. *Earthquake Engineering & Structural Dynamics*, **31** (4), 955-976.

[3] Whittle J, Williams M, Karavasilis TL, Blakeborough A (2012): A comparison of viscous damper placement methods for improving seismic building design. *Journal of Earthquake Engineering*, **16** (4), 540-560.

[4] Zhang RH, Soong TT (1992): Seismic design of viscoelastic dampers for structural applications. *Journal of Structural Engineering*, **118** (5), 1375-1392.

[5] Takewaki I (1997): Optimal damper placement for minimum transfer functions. *Earthquake Engineering & Structural Dynamics*, **26** (11), 1113-1124.

[6] Lopez-Garcia D (2001): A simple method for the design of optimal damper configurations in MDOF structures. *Earthquake Spectra*, **17** (3), 387-398.

[7] Lavan O, Levy R (2006): Optimal design of supplemental viscous dampers for linear framed structures. *Earthquake Engineering & Structural Dynamics*, **35** (3), 337-356.

[8] Lin JL, Bui MT, Tsai KC (2014): An energy-based approach to the generalized optimal locations of viscous dampers in two-way asymmetrical buildings. *Earthquake Spectra*, **30** (2), 867-889.

[9] Tubaldi E, Barbato M, Dall'Asta A (2014): Performance-based seismic risk assessment for buildings equipped with linear and nonlinear viscous dampers. *Engineering Structures*, **78**, 90-99.

[10] Gidaris I, Taflanidis AA (2015): Performance assessment and optimization of fluid viscous dampers through life-cycle cost criteria and comparison to alternative design approaches. *Bulletin of Earthquake Engineering*, **13** (4), 1003-1028.

[11] Pollini N, Lavan O, Amir O (2016): Towards realistic minimum-cost optimization of viscous fluid dampers for seismic retrofitting. *Bulletin of Earthquake Engineering*, **14** (3), 971-998.

[12] Taflanidis AA, Scruggs JT (2010): Performance measures and optimal design of linear structural systems under stochastic stationary excitation. *Structural Safety*, **32** (5), 305-315.

[13] Di Paola M, Navarra G (2009): Stochastic seismic analysis of MDOF structures with nonlinear viscous dampers. *Structural Control and Health Monitoring*, **16** (3), 303-318.

[14] Lutes LD, Sarkani S (2004): *Randon Vibrations – Analysis of Structural and Mechanical Systems*. Elsevier.

[15] Der Kiureghian A (1980): Structural response to stationary excitation. *Journal of Engineering Mechanics*, **106** (EM6), 1195-1213.

[16] Roberts JB, Spanos PD (2003): *Random Vibration and Statistical Linearization*. Dover.

[17] Holmstrom K, Goran AO, Edvall MM (2009): *User's guide for TOMLAB 7*. Tomlab Optimization Inc. (www.tomopt.com/tomlab/).

[18] Ugalde D, Parra PF, Lopez-Garcia D (2019): Assessment of the seismic capacity of tall wall buildings using nonlinear finite element modeling. *Bulletin of Earthquake Engineering*, **17** (12), 6565-6589.

[19] Clough RW, Penzien J (1993): *Dynamics of Structures*. Computers and Structures, 2nd edition.

Appendix

The state-space representation of the structure in Eq (1) is:

$$\dot{\mathbf{x}}_{ss}(t) = \mathbf{A}_s \mathbf{x}_{ss}(t) + \mathbf{B}_s \mathbf{f}_d(t) + \mathbf{E}_s \ddot{x}_g(t), \qquad \mathbf{z}(t) = \mathbf{C}_s \mathbf{x}_{ss}(t) + \mathbf{D}_s \mathbf{f}_d(t) \tag{17}$$

where $\mathbf{x}_{ss} \in \Re^{2n}$ is the state vector collecting relative to the ground displacements and velocities of all stories $\mathbf{x}_{ss} = [\mathbf{x}_s^T \quad \dot{\mathbf{x}}_s^T]^T$, and the matrices in Eq. (17) are defined as:

$$\mathbf{A}_s = \begin{bmatrix} \mathbf{0}_{n_s x n_s} & \mathbf{I}_{n_s} \\ -\mathbf{M}_s^{-1}\mathbf{K}_s & -\mathbf{M}_s^{-1}\mathbf{C}_s \end{bmatrix} \mathbf{B}_s = \begin{bmatrix} \mathbf{0}_{n_s x n_d} \\ -\mathbf{T}_d^T \end{bmatrix} \mathbf{E}_s = \begin{bmatrix} \mathbf{0}_{n_s x 1} \\ -\mathbf{R}_s \end{bmatrix} \mathbf{C}_s = \begin{bmatrix} \mathbf{T}_s & \mathbf{0}_{n_s x n_s} \\ -\mathbf{M}_s^{-1}\mathbf{K}_s & -\mathbf{M}_s^{-1}\mathbf{C}_s \end{bmatrix} \mathbf{D}_s = \begin{bmatrix} \mathbf{0}_{n_s x n_d} \\ -\mathbf{M}_s^{-1}\mathbf{T}_d^T \end{bmatrix} \tag{18}$$

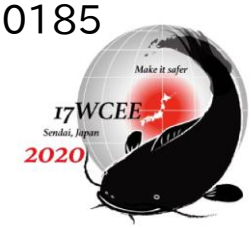

In the above expressions, the output matrix $\mathbf{C}_s$ accounts for output variables vector **z** that includes inter-story drifts and absolute accelerations for all floors. Further, $\mathbf{I}_a$ is the identity matrix of dimension a, $\mathbf{0}_{axb}$ is the zero matrix of dimensions axb, $\mathbf{T}_s$ is a transformation matrix defining relative responses between consecutive floors (i.e., a square matrix with dimension n_s with 1 in the diagonal and -1 in the first off-diagonal). Combining Eqs. (17) and (2) leads to the representation in Eq. (3) where:

$$\mathbf{x}=\begin{bmatrix}\mathbf{x}_{ss}\\ \mathbf{x}_q\end{bmatrix} \quad \mathbf{A}=\begin{bmatrix}\mathbf{A}_s & \mathbf{E}_s\mathbf{C}_q\\ \mathbf{0}_{n_q x 2n_s} & \mathbf{A}_q\end{bmatrix} \quad \mathbf{B}=\begin{bmatrix}\mathbf{B}_s\\ \mathbf{0}_{n_q x n_d}\end{bmatrix} \quad \mathbf{E}=\begin{bmatrix}\mathbf{0}_{2n_s x 1}\\ \mathbf{E}_q\end{bmatrix} \quad \mathbf{C}=\begin{bmatrix}\mathbf{C}_s & \mathbf{0}_{n_z x n_q}\end{bmatrix} \quad \mathbf{D}=\begin{bmatrix}\mathbf{D}_s & \mathbf{0}_{n_z x n_q}\end{bmatrix} \tag{19}$$

Also, the state connectivity matrix corresponds to:

$$\mathbf{L}_d=\begin{bmatrix}\mathbf{0}_{n_d x n_s} & \mathbf{T}_d & \mathbf{0}_{n_d x n_f}\end{bmatrix} \tag{20}$$

Lastly, the state-space matrices of the excitation model used in the case study is:

$$\mathbf{A}_q=\begin{bmatrix}0 & 1 & 0 & 0\\ -\omega_g^2 & -2\zeta_g\omega_g & 0 & 0\\ 0 & 0 & 0 & 1\\ -\omega_g^2 & -2\zeta_g\omega_g & -\omega_f^2 & -2\zeta_f\omega_f\end{bmatrix} \quad \mathbf{E}_q=\begin{bmatrix}0\\1\\0\\0\end{bmatrix} \quad \mathbf{C}_q=\sigma_o\begin{bmatrix}-\omega_g^2 & -2\zeta_g\omega_g & \omega_f^2 & 2\zeta_f\omega_f\end{bmatrix} \tag{21}$$

where σ_o is chosen such that the excitation has the desired a_{RMS} intensity.

